NANO LETTERS

2005
Vol. 5, No. 7
1463−1468

Local Charge Transport in Two-Dimensional PbSe Nanocrystal Arrays Studied by Electrostatic Force Microscopy

Zonghai Hu, Michael D. Fischbein, and Marija Drndić*

Department of Physics and Astronomy, University of Pennsylvania, Philadelphia, Pennsylvania 19104

Received May 4, 2005; Revised Manuscript Received June 8, 2005

ABSTRACT

Two-dimensional PbSe nanocrystal arrays on silicon nitride membranes were investigated using electrostatic force microscopy (EFM) and transmission electron microscopy (TEM). Changes in lattice and transport properties upon annealing in a vacuum were revealed. Local charge transport behavior was directly imaged by EFM and correlated to nanopatterns observed with TEM. Charge transport through nanochannels in complex two-dimensional nanocrystal networks was identified. Our results demonstrate the importance of measurements of local transport details complementary to the conventional current–voltage (*I*–*V*) measurements.

Nanocrystals (NCs), also called "artificial atoms", have been receiving a great deal of attention because of their interesting properties which can be tuned by controlling their size and shape.[1,2] For example, size-dependent quantum confinement effects are readily observed, especially in the IV−VI class of NCs, because their exciton Bohr radii are in the nanometer range.[3,4] Arrays of NCs also exhibit rich physics and may be thought of as "artificial solids". For instance, a reversible metal−insulator transition was observed in Langmuir films of colloidal Ag NCs by tuning the separation between the NCs.[5] NC arrays have become a new class of materials with potential applications including light-emitting devices,[6] remote sensors in the microwave regime,[7] photovoltaic cells,[8] thermoelectrics,[9] and biosensors.[10]

Recently developed synthetic techniques for producing NC assemblies with well-controlled particle size, shape, and interdot spacing have made the systematic study of their electrical and optical properties possible. Previous transport measurements on arrays of metallic and doped semiconducting NCs have revealed them to be quite conductive[11] while measurements on as-deposited arrays of undoped semiconducting NCs have shown that they are insulating (see for example refs 12 and 16). In the case of undoped semiconducting NCs, it is believed that long-range Coulomb interactions between charges on different NCs and charge trapping slow the carrier transfer dynamics. Annealing has been proven to be an effective way to increase the conductivity of NC arrays while decreasing the interdot separation.[12,13]

Conventional current−voltage (*I*−*V*) measurements are highly valuable. However, they typically only probe collective transport properties of the entire array. Little information is revealed about the local transport behavior around features such as defects and impurities. Such information is crucial for device applications and for uncovering the mechanisms involved in array transport in general. Electrostatic force microscopy (EFM) is a technique for probing local charge distributions on surfaces with high spatial resolution. EFM is therefore capable of resolving many issues that arise from restricting transport measurements to *I*−*V* characteristics. Interesting EFM results of local charge transport in carbon nanotubes have been reported recently.[14]

Here we present a combined electrostatic force microscopy and transmission electron microscopy (EFM/TEM) investigation of charge transport in PbSe NC arrays. In this study, EFM and TEM were performed on the same positions of the same NC arrays to achieve a more comprehensive understanding of these systems. Both as-deposited and annealed two-dimensional (2D) PbSe NC arrays were studied. The as-deposited PbSe NC arrays were found to be insulating. Mild annealing in a vacuum was found to improve the array ordering, to reduce the separation between NCs, and to dramatically enhance the conductivity of the arrays. Good correlation between local charge transport behavior, observed with EFM, and the nanopatterns in the PbSe array, imaged by TEM, was demonstrated. Our results show the importance of studying the local charge transport in addition to the collective transport of the entire NC array and

* Corresponding author. E-mail: drndic@physics.upenn.edu.

10.1021/nl050828p CCC: $30.25
Published on Web 06/21/2005

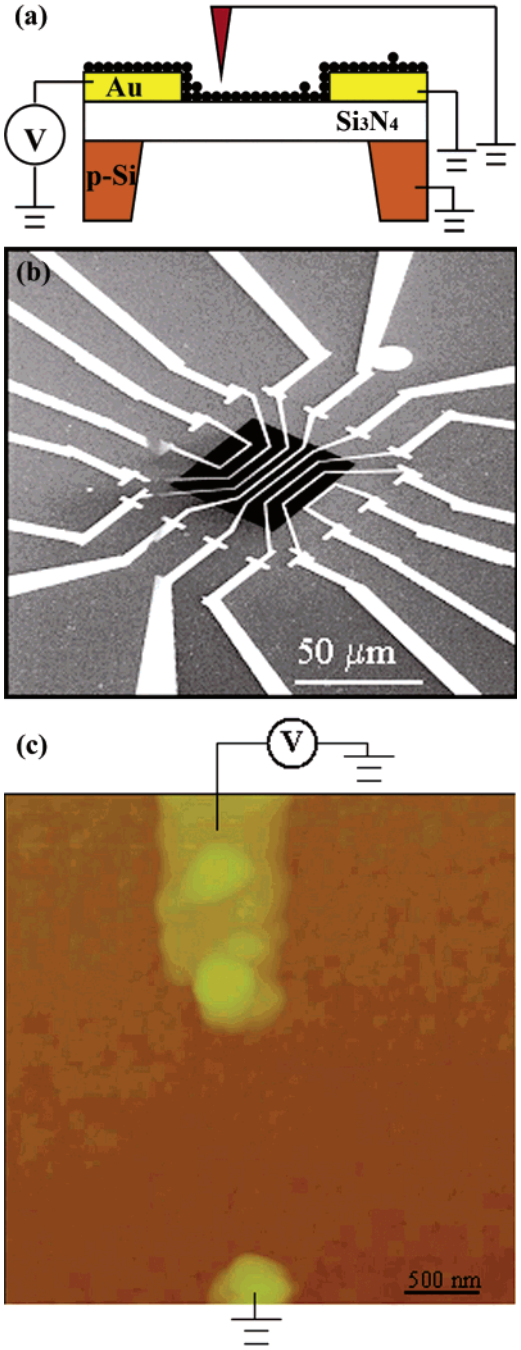

Figure 1. (a) Schematic diagram of the experimental setup. (b) Scanning electron micrograph of the device. The white features are Au electrodes. The black square in the center is the silicon nitride membrane window with eight pairs of electrodes. (c) Atomic force microscopy height image of the area under study. The bias was applied to the top electrode. The bottom electrode was grounded at all times.

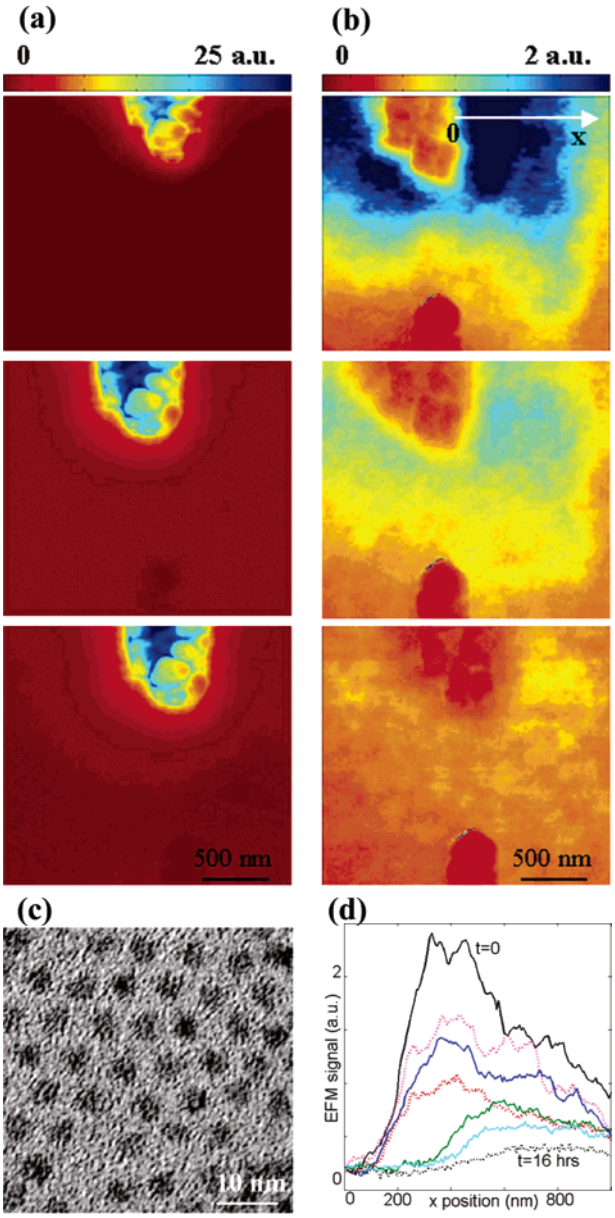

Figure 2. (a) Electrostatic force microscopy (EFM) images taken at $t = 0$, 8, and 16 h, respectively, while applying a -6 V bias to the top electrode (see Figure 1c). (b) EFM images taken at $t = 0$, 8, 16 h, respectively, after the bias on the top electrode was switched back to zero. Notice that the EFM signals during discharging are on a smaller scale than that of charging. (c) TEM micrograph showing the as-deposited superlattice. (d) The line profile of the EFM signal along the fixed line marked in (b) over time at $t = 0$, 2, 4, 6, 8, 12, and 16 h, from top to bottom curve, respectively; $x = 0$ is set at the edge of the top electrode as marked in (b).

demonstrate that combined EFM/TEM is a powerful tool for this purpose. The EFM/TEM technique has the potential to track charge transport through nanochannels even in a complex NC network.

Figure 1 illustrates the experimental setup. As shown in Figure 1a, the devices used consisted of a 100 nm thick layer of silicon nitride (Si_3N_4) on top of a Si substrate. Si was removed from beneath the Si_3N_4 in a 50 μm $\times$ 50 μm square, leaving the Si_3N_4 as a free-standing membrane in this area. Au/Cr electrodes 60 nm thick were lithographically fabricated on top of the Si_3N_4 as shown in Figure 1b. The gap between each pair of electrodes is $\sim$1 μm long as shown in Figure 1c. Performing measurements on a thin Si_3N_4 membrane enabled us to do combined EFM/TEM studies on the same device. Furthermore, undesirable effects caused by charges located at the Si_3N_4/Si interface were eliminated.[15] PbSe NCs (3.5 nm diameter with a 5% size distribution) with $\sim$2 nm oleic acid capping were drop casted from a diluted 9:1 hexane/octane solvent onto the device. Immediately after drop casting the NCs, the device was placed into the EFM

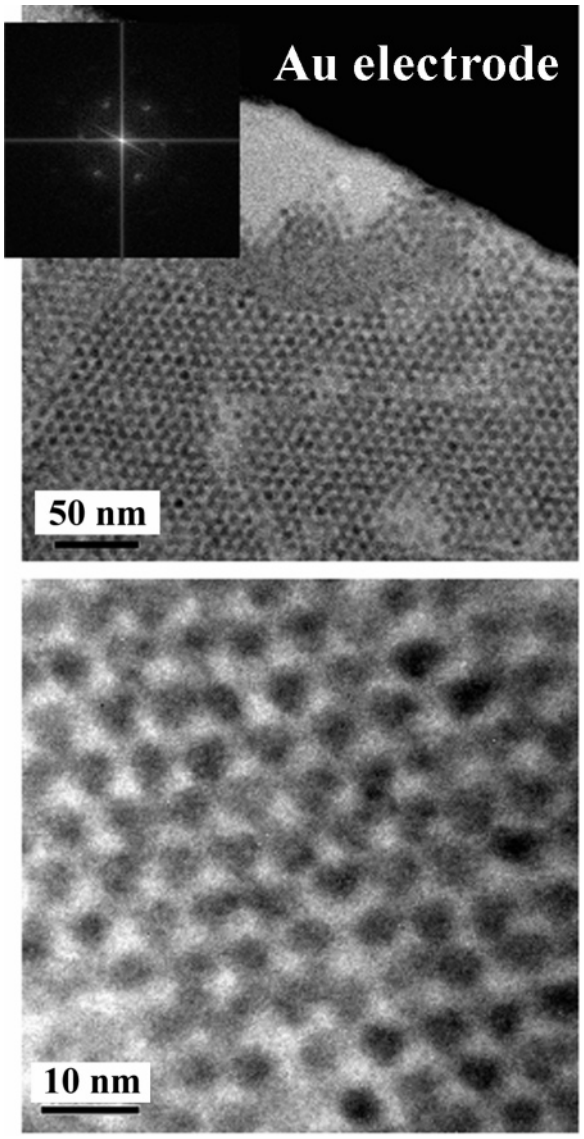

Figure 3. Transmission electron micrographs taken after annealing of the NC array at 420 K for 4 h in a vacuum. The inset is the Fourier transform power spectrum of the NC superlattice in the area shown.

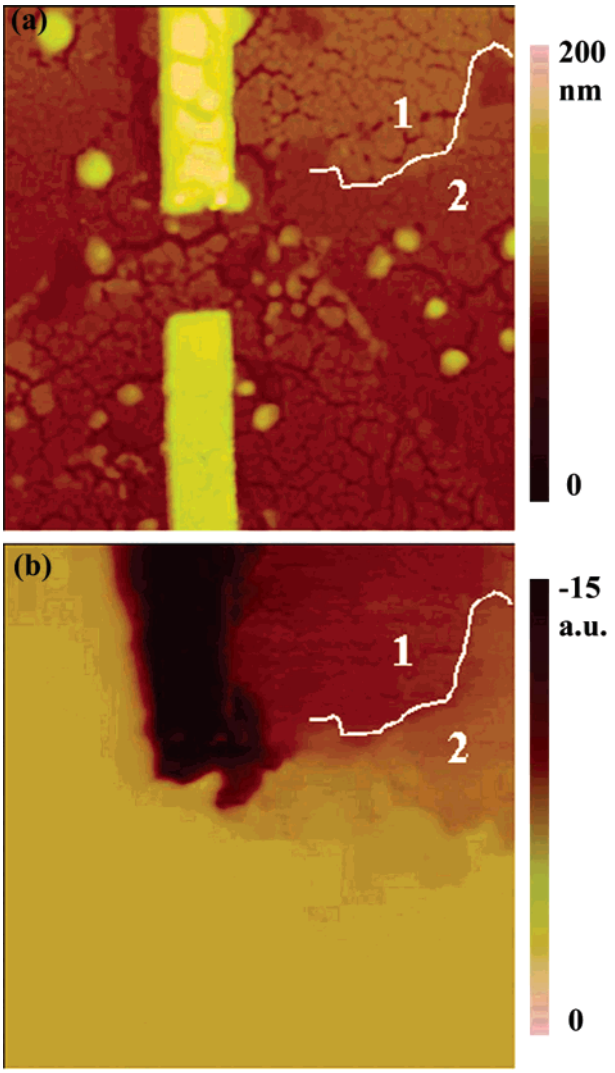

Figure 4. 5 μm × 5 μm AFM height image (a) and corresponding EFM image (b) taken immediately after a −6 V bias between the electrodes was switched on the top electrode after annealing. The bottom electrode was grounded at all times.

measurement chamber which was then quickly pumped down to lower than 1×10^{-5} Torr. The exposure time to air was less than 3 min, which was sufficiently short to avoid oxidation or degradation of the NCs. All later treatments to the NCs were carried out *in situ* inside the EFM chamber.

Electrostatic force microscopy (EFM) is a technique developed on the basis of atomic force microscopy (AFM). During EFM measurements, every line of the sample surface is scanned twice. The first scan operates in the normal AFM tapping mode and records the topography of the sample. During the second scan, the tip is lifted to a specified height (typically 30 nm in our measurements) and follows the height contour obtained in the first scan while a bias is applied between the tip and the surface. The electrostatic force between the tip and the surface is given approximately by

$$F = Q_s^2/4\pi\epsilon_0 z^2 + Q_s CV/4\pi\epsilon_0 z^2 + \mathrm{d}C/\mathrm{d}z\, V^2/2$$

where Q_s is the surface charge, ϵ_0 is the vacuum dielectric constant, z is the tip−surface separation, C is the capacitance between the tip and the surface, and V is the potential difference between the tip and the surface. When $V = 0$, the EFM signal, which is the change in the resonant frequency of the cantilever, is proportional to Q_s^2.[16] From EFM signals induced by local potential and charge density, information about local transport properties can be obtained.

Our AFM operates in a vacuum chamber where the sample holder can be heated. As-deposited 2D NC arrays were first measured with EFM and subsequently annealed *in situ* at temperatures up to 420 K. After slowly cooling to room temperature, EFM/TEM studies were carried out on the annealed arrays.

Parts a and b of Figure 2 show EFM images taken over time when a $V = -6$ V bias was applied across the two electrodes (charging process) and when the bias was switched off (discharging process), respectively. The bottom electrode barely appears in the EFM images because it was grounded throughout the measurement. The bias was applied to the top electrode and it appears darkest. Regions in the gap

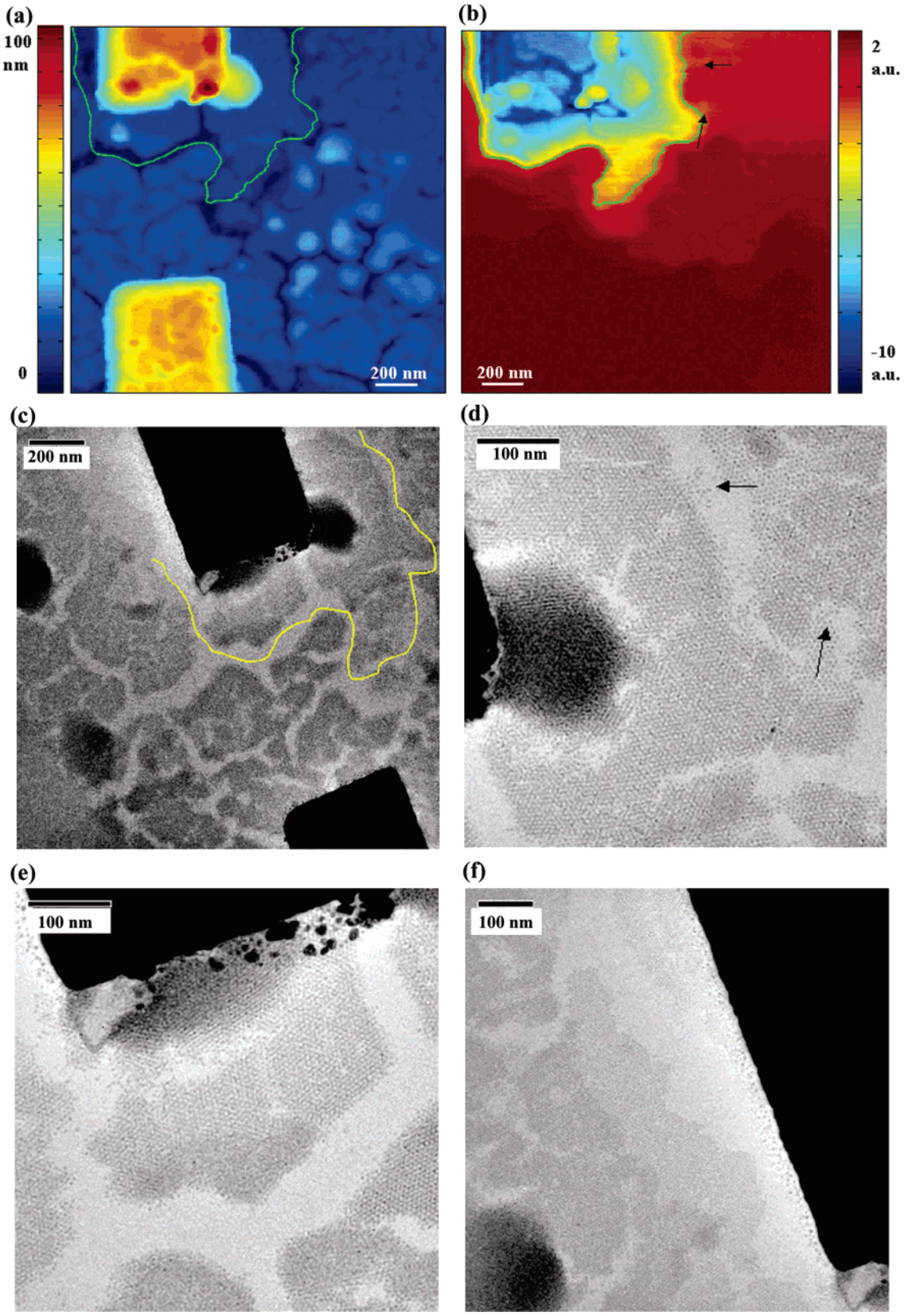

Figure 5. (a) 2 μm $\times$ 2 μm AFM height image and (b) corresponding 2 μm $\times$ 2 μm EFM image showing the NC terraces and cracks in the NC film around the electrodes. (c−f) TEM micrographs showing different areas around the electrodes: (c) the same area between the two electrodes as in (a) and (b); (d) the area around the right corner of the top electrode; (e) the area around the left corner of the top electrode; (f) the area along the left edge of the top electrode.

became darker over time in a pattern roughly following the potential contour between the two electrodes, indicating that the PbSe NC array was gradually charging. The charging process was very slow, and the current did not reach a steady

state after 16 h of charging. This indicated that the as-deposited PbSe NC array was insulating, which agrees with previous reports on other semiconducting NC arrays.[16] After discharge for the same amount of time, some residual charges were still detected in EFM, indicating that the discharging process could be even slower than charging. Figure 2d shows the EFM signal profile recorded over time along the fixed line marked in Figure 2b. Applying an analysis similar to what is described in ref 16 to the data shown in Figure 2d yielded a charge diffusion coefficient for the discharging process that was below 10^{-15} m^2/s, which is much smaller than the diffusion coefficient of the PbSe bulk material, $\sim 10^{-2}$ m^2/s. We believe this large resistance is due to the large spacing and weak coupling between NCs in the as-deposited undoped array, as is shown in the TEM micrograph in Figure 2c.

Figure 3 is a TEM micrograph of a sample which had been annealed in a vacuum at 420 K for 4 h. The inset is a Fourier transform power spectrum of the same area showing clear peaks that correspond to the highly ordered hexagonal NC superlattice. While the size of the PbSe NC core was unaffected by the annealing, the spacing between NCs decreased from ~3 nm on average in the as-deposited array to ~2 nm on average in the annealed array. This clearly demonstrates the mobility of the deposited "dry" NCs at elevated temperature. A similar effect was observed in CdSe NC arrays annealed in nitrogen.[12] These results show that annealing is an effective way of reducing the separation between NCs. The details of the NC dynamics during the annealing process are still under investigation.[17]

AFM height images of the NC array were also taken after annealing. Figure 4a is a typical height image showing that the NC array was not uniform in thickness after the annealing. Instead, sectional analysis revealed that the array consisted of terraces of one to five monolayers of PbSe NCs. For example, terraces in region 1 in Figure 4a consisted of three monolayers, while terraces in region 2 consisted of two monolayers. Some terraces were continuous in space, while other adjacent terraces were apparently separated by "nano-cracks" formed during annealing, in which few or no NCs existed.

Figure 4b shows an EFM image taken immediately after a −6 V bias was applied across the annealed PbSe array between the two electrodes. Terraces of NCs even far away from the top electrode charged instantaneously, indicating that the conductivity of the NC array was dramatically enhanced. However, the charging pattern was highly anisotropic. It did not follow the front of the expected potential profile between the two electrodes as it did in the NC array before annealing. Some of these charging patterns can be easily understood by comparing the EFM image with its corresponding topography image, which is shown in Figure 4a. For instance, the EFM image shows region 1 as being darker than region 2, and since the AFM topography shows region 1 to be thicker than region 2, this difference in charge density is explained if it is assumed that all the individual NCs were charged uniformly.

Higher resolution AFM, EFM, and TEM images of the same annealed NC array are shown in parts a, b, and c of Figure 5, respectively. One distinct contour of constant EFM signal was marked in Figure 5a and superimposed on the AFM height image and on the TEM micrograph. Upon comparison of the figures, a clear correlation can be seen between the EFM contour and the cracks surrounding the top electrode revealed in the AFM and TEM images. Apparently, these cracks greatly hindered charge transfer and caused sharp contrast across the contour in the EFM signal. The TEM micrograph displayed in Figure 5e shows that there were indeed almost no NCs in the cracks and therefore explains the absence of conduction across them.

In several regions, thin channels of PbSe NCs, as narrow as 20 nm wide, actually extended completely across a crack. An example of this situation is indicated with arrows in the TEM image shown in Figure 5d. The charge transport patterns around these nanochannels are discernible in the corresponding EFM signal, as is indicated in Figure 5b. This result exemplifies the ability of the combined EFM/TEM approach to track local charge transport around nanometer scale features even in a complex network of nanopatterns.

The formation of these cracks most likely occurs during annealing, but their size may increase throughout the period of being in the EFM chamber under vacuum. This resulted in many completely disconnected regions within the array. In a sense, these cracks act like defects in ordinary solid materials. Their presence could certainly affect many characteristics measured in conventional $I-V$ experiments. Our results demonstrate the importance of using microscopic techniques to investigate the local details of transport in 2D NC systems.

In summary, we report on combined and correlated EFM and TEM studies of 2D NC arrays. Charge transport in insulating and semiconducting 2D PbSe NC arrays was directly imaged by EFM. Good correlation between the local charge transport patterns and the topographical features as small as 20 nm shown in TEM were found. Our results demonstrate that this 2-fold technique is useful for obtaining detailed information about local transport properties. Annealing in a vacuum was observed to be an effective method for controlling the interdot coupling and the resulting collective properties of NC arrays.

Acknowledgment. We are grateful for support by the ONR Young Investigator Award (N000140410489), the American Chemical Society (ACS) PRF award (41256-G10), and in part, the NSF Career Award DMR-0449553 and NSF MRSEC DMR00-79909. M.F. acknowledges funding from the NSF-IGERT program (Grant DGE-0221664).

References

(1) Murray, C. B.; Kagan, C. R.; Bawendi, M. G. *Annu. Rev. Mater. Sci.* **2000**, *30*, 545 and references therein.
(2) Alivisatos, A. P. *J. Phys. Chem.* **1996**, *100*, 13226 and references therein.
(3) Du, H.; Chen, C.; Krishnan, R.; Kraus, T. D.; Harbold, J. M.; Wise, F. W.; Thomas, M. G.; Silcox, J. *Nano Lett.* **2002**, *2*, 1321.

(4) Wehrenberg, B. L.; Wang, C.; Guyot-Sionnest, P. *J. Phys. Chem. B* **2002**, *106*, 10634.
(5) Collier, C. P.; Saykally, R. J.; Shiang, J. J.; Henrichs, S. E.; Heath, J. R. *Science* **1997**, *277*, 1978.
(6) Colvin, V. L.; Schlamp, M. C.; Alivisatos, A. P. *Nature* **1994**, *370*, 354.
(7) Kim, S. H.; Markovich, G.; Rezvani, S.; Choi, S. H.; Wang, K. L.; Heath, J. R. *Appl. Phys. Lett.* **1999**, *74*, 317.
(8) Huynh, W. U.; Dittmer, J. J.; Teclemarian, N.; Milliron, D. J.; Alivisatos, A. P.; Barnham, K. W. J. *Phys. Rev. B* **2003**, *67*, 115326.
(9) Q, X.; Zhu, J.; Pu, L.; Shi, Y.; Zheng, Y.; Chen, H. *Inorg. Chem. Commun.* **2004**, *7*, 319.
(10) Murphy, C. J.; Brauns, E. B.; Gearheart, L. In *Advances in Microcrystalline and Nanocrystalline Semiconductors*; Symposium, Materials Research Society: Pittsburgh, PA, 1997; p 597.
(11) Yu, D.; Wang, C.; Wehrenberg, B. L.; Guyot-Sionnest, P. *Phys. Rev. Lett.* **2004**, *92*, 216802.
(12) Drndic, M.; Jarosz, M. V.; Morgan, N. Y.; Kastner, M. A.; Bawendi, M. G. *J. Appl. Phys.* **2002**, *92*, 7498.
(13) Black, C. T.; Murray, C. B.; Sandstrom, R. L.; Sun, S. H. *Science* **2000**, *290*, 1131.
(14) Freitag, M.; Johnson, A. T.; Kalinin, S. V.; Bonnell, D. A. *Phys. Rev. Lett.* **2002**, *89*, 216801.
(15) Ben-Porat, C. H.; Cherniavskaya, O.; Brus, L.; Cho, K. S.; Murray, C. B *J. Phys. Chem. A* **2004**, *108*, 7814.
(16) Drndic, M.; Markov, R.; Jarosz, M. V.; Bawendi, M. G.; Kastner, M. A.; Markovic, N.; Tinkham, M. *Appl. Phys. Lett.* **2003**, *83*, 4008.
(17) Perez-Dieste, V.; Castellini, O.M.; Crain, J. N.; Eriksson, M. A.; Kirakosian, A.; Lin, J. L.; McChesney, J. L.; Himpsel, F. L.; Black, C. T.; Murray, C. B. *Appl. Phys. Lett.* **2003**, *83*, 5053.

NL050828P